



THE UNIVERSITY *of* EDINBURGH

Edinburgh Research Explorer

Physiological controls of the isotopic time lag between leaf assimilation and soil CO₂ efflux

Citation for published version:

Salmon, Y, Barnard, RL & Buchmann, N 2014, 'Physiological controls of the isotopic time lag between leaf assimilation and soil CO₂ efflux', *Functional Plant Biology*. <https://doi.org/10.1071/FP13212>

Digital Object Identifier (DOI):

[10.1071/FP13212](https://doi.org/10.1071/FP13212)

Link:

[Link to publication record in Edinburgh Research Explorer](#)

Document Version:

Peer reviewed version

Published In:

Functional Plant Biology

Publisher Rights Statement:

© CSIRO PUBLISHING 2014

General rights

Copyright for the publications made accessible via the Edinburgh Research Explorer is retained by the author(s) and / or other copyright owners and it is a condition of accessing these publications that users recognise and abide by the legal requirements associated with these rights.

Take down policy

The University of Edinburgh has made every reasonable effort to ensure that Edinburgh Research Explorer content complies with UK legislation. If you believe that the public display of this file breaches copyright please contact openaccess@ed.ac.uk providing details, and we will remove access to the work immediately and investigate your claim.



1 **Title: Physiological controls of the isotopic time lag between leaf assimilation and soil**
2 **CO₂ efflux**

3 Running title: Physiological controls of C transfer belowground

4
5 Yann Salmon^{1,2,3*}, Romain L. Barnard^{1,4}, Nina Buchmann¹

6
7 ¹ Institute of Agricultural Sciences, ETH Zurich, 8092 Zurich, Switzerland

8 ² Institute of Evolutionary Biology and Environmental Studies, University of Zurich, 8057
9 Zurich, Switzerland

10 ³ present address: Global Change Institute, The University of Edinburgh, Crew Building, The
11 King's Buildings, West Mains Road, Edinburgh EH9 3JF, UK

12 ⁴ present address: INRA, UMR1347 Agroécologie, 17 rue Sully, BP 86510, Dijon, France

13 * Corresponding author

14 Date received: _____

15 Word count: 5567

16 Introduction: 587, Materials and Methods: 2260, Results: 683, Discussion and conclusion:
17 1997, and Acknowledgements: 40. Figures: 4, Tables: 2

18 Correspondence: Yann Salmon

19 Phone: +44 (0) 131 651 7034

20 Fax: +44 (0) 131 662 0478

21 Email: yann.salmon@ed.ac.uk

22

23 **Summary for table of contents**

24 The dynamics of recently-assimilated carbon are a key driver of the carbon budget of
25 terrestrial ecosystems and of their response to global change. Our study shows that
26 belowground transfer of photosynthates is related to plant physiological controls, which,
27 unlike environmental controls, are still poorly characterized. Our study contributes to
28 improve the understanding of the dynamics of carbon allocation and isotopic signatures in
29 terrestrial ecosystems.

30 **Abstract**

31 Environmental factors and physiological controls on photosynthesis influence the carbon
32 isotopic signature of ecosystem respiration. Many ecosystem studies have used stable carbon
33 isotopes to investigate environmental controls on plant carbon transfer from above- to
34 belowground. However, a clear understanding of the internal mechanisms underlying time-
35 lagged responses of carbon isotopic signatures in ecosystem respiration to environmental
36 changes is still lacking. This study addressed plant physiological controls on the transfer time
37 of recently assimilated carbon from assimilation to respiration. We produced a set of six
38 wheat plants with varying physiological characteristics, by growing them under a wide range
39 of nitrogen supply and soil water content levels under standardized conditions. The plants
40 were pulse-labelled with $^{13}\text{C}\text{-CO}_2$, and the isotopic signature of CO_2 respired in the dark by
41 plants and soil was monitored continuously over two days. Stomatal conductance (g_s) was
42 strongly related to the rate of transfer of recently assimilated carbon belowground. The higher
43 g_s , the faster newly assimilated carbon was allocated belowground and the faster it was
44 respired in the soil. Our results suggest that carbon sink strength of plant tissues may be a
45 major driver of transfer velocity of recently assimilated carbon to plant respiratory tissues and
46 soil respiration.

47

48 **Keywords**

49 Respiration, transpiration, stable carbon isotopes, carbon transfer, ^{13}C , photosynthates

50

51

52 **Introduction**

53

54 Improving our understanding of the fate of recently assimilated carbon (C), the
55 variability of its allocation to above- and belowground ecosystem compartments, as well as
56 its respiratory losses to the atmosphere is essential to estimate and model the sensitivity of the
57 global terrestrial C budget under changing environmental conditions (Litton *et al.* 2007). In
58 particular, determining the velocity and the quantity of recently assimilated C allocated to
59 different ecosystem components is a crucial step to improve our understanding of C dynamics
60 in terrestrial ecosystems (Kuzyakov and Gavrichkova 2010).

61 Using stable isotopes as tracers allows one to follow photosynthates from source
62 organs to CO₂ respired by different organisms in terrestrial ecosystems (Dawson *et al.* 2002;
63 Brüggemann *et al.* 2011; Epron *et al.* 2012). Under natural conditions, changes in
64 photosynthetic discrimination (Δ) imprint the carbon isotope composition ($\delta^{13}\text{C}$) of new
65 photoassimilates, as leaf physiology responds to environmental conditions (Farquhar *et al.*
66 1989), which can then be tracked in the plant until these photoassimilates are respired. The
67 time lag between changes in Δ and associated changes in $\delta^{13}\text{C}$ of respired CO₂, later referred
68 to as isotopic time lag, has often been used to understand the impact of environmental
69 variables on the C cycle (see reviews by Kuzyakov and Gavrichkova 2010; Mencuccini and
70 Hölttä 2010; Brüggemann *et al.* 2011). However, recent studies have challenged the
71 simplicity of these time-lagged responses, by shedding light on diel variations of $\delta^{13}\text{C}$ in
72 respired CO₂, post-photosynthetic and respiration fractionation, damping of the ¹³C signal as
73 it is transferred belowground, all of which contributing to blur the time lag from assimilation
74 to respiration (Gessler *et al.* 2008; Kodama *et al.* 2008; Werner and Gessler 2011). It has
75 become increasingly clear in the last decade that investigating the isotopic time lag responses

76 to external, i.e., environmental drivers should not neglect the internal drivers, i.e. plant
77 physiology.

78 Plant biochemistry and physiology play a major role in C allocation and particularly
79 in the transfer of C from above to belowground, affecting the isotopic time lag through its
80 three main components: velocity of C transfer, quantity of C transferred to different organs,
81 and substrate identity carrying the isotopic signal (Paul and Foyer 2001; Brüggemann *et al.*
82 2011). We expect that frequent measurements in plant-soil systems that cover a range of
83 environmental and physiological conditions, but in which day-to-day environmental
84 conditions remain constant, should shed light on the physiological drivers underlying changes
85 in rate of C transfer belowground and $\delta^{13}\text{C}$ of respired CO_2 .

86 The present study avoided day-to-day environmental variability to address plant
87 physiological controls on the transfer time of recently assimilated C, from leaf assimilation to
88 above- and belowground respiration. A set of wheat plants with varying physiological
89 characteristics was produced by growing them under a wide range of nitrogen (N) supply and
90 soil water resource levels, two resources known to be of major importance for plant
91 physiological status (Poorter and Nagel 2000), while all other environmental conditions were
92 standardized and kept constant on a day-to-day basis. The plants were pulse-labelled with
93 $^{13}\text{CO}_2$, and the isotopic signatures of CO_2 respired by aboveground biomass (i.e., leaves, leaf
94 sheath and extremely small stem, further referred to as shoot; $\delta^{13}\text{C}_{\text{R-shoot}}$) and by soil ($\delta^{13}\text{C}_{\text{R-soil}}$)
95 were monitored over two days in the dark. The release of ^{13}C label by shoot and soil
96 respiration was related to plant physiological variables to identify the most relevant
97 physiological drivers of short-term rate of C transfer belowground. We hypothesized that the
98 isotopic time lag would be shorter in plants with higher photosynthetic activity and higher
99 transpiration rates.

100

101 **Material and methods**

102

103 **Experimental setup**

104 Wheat plants (*Triticum aestivum* L.) were grown under different N and soil water
105 resource levels, in order to create plants covering a wide physiological status range. Square
106 pots (18x18x17 cm height) were filled with a 2:1 mixture of vermiculite and sieved (1 cm
107 mesh) clay loam soil (28.5% organic matter, pH 6.8, texture of inorganic matter: 30% clay,
108 41.8% silt, 28.2% sand). Seeds were germinated on a thin layer of soil. One week after
109 germination, the plantlets were transferred in the pots, following an even pattern (16
110 individuals per pot, i.e., 658 plants m⁻²) on three quarters of the pot surface. A PVC
111 (polyvinyl chloride) soil collar (7 cm diameter, 5 cm high) for soil CO₂ efflux measurements
112 was inserted 2.5 cm deep in the remaining quarter of the pot surface area.

113 Plants were grown under controlled conditions in a growth chamber (PGV36,
114 Conviron, Winnipeg, Canada). The pots were rotated weekly to avoid position effects in the
115 chamber. Chamber conditions followed a 14h photoperiod (photosynthetically active
116 radiation, PAR, of ca. 400 μmol m⁻² s⁻¹) with day/night temperatures of 20°C/15°C,
117 respectively. CO₂ concentrations were maintained at app. 400 μmol mol⁻¹ and air humidity
118 between 60 and 70%. Leaves of well-watered *Zea mays* L. were used as phytometers to
119 provide an integrated ¹³C signature of background CO₂ in the chambers, since the ¹³C
120 discrimination of C₄ species is relatively constant under non-limiting conditions (Evans *et al.*
121 1986; Buchmann *et al.* 1996). Phytometer leaf biomass was sampled every two weeks, dried
122 and finely ground prior to isotope ratio analysis (see below). Direct measurements of δ¹³C of
123 CO₂ in the chamber atmosphere were made on a biweekly basis to validate the range of δ¹³C
124 of background CO₂ obtained from the phytometer results.

125 Different resource level combinations of N and soil water were applied during two

126 months. We used a full factorial combination of two fertilization levels (non-fertilized, plants
127 1, 2 and 3 and fertilized plants 4, 5 and 6) and three soil water content (SWC) levels (47%,
128 plants 1 and 4; 63%, plants 2 and 5; and 71%, plants 3 and 6). N fertilization consisted of a
129 daily input of 20 ml of a 5 g N L⁻¹ solution (N:P:K 1:0.4:0.6, Wuxal[®] Liquid, AgNova
130 Technologies Pty Ltd, Victoria, Australia). Daily weighing and watering of the pots to exactly
131 compensate water losses due to evapotranspiration ensured the accuracy of the water resource
132 level. Two pots were used for each combination of resource levels. After two months of
133 growth, one pot was used for ecophysiological measurements, to assess plant physiological
134 status. The other pot was used for ¹³C labelling of the plant and subsequent measurements of
135 $\delta^{13}\text{C}_{\text{R-soil}}$ and $\delta^{13}\text{C}_{\text{R-shoot}}$ in the dark for two days, which were related to the ecophysiological
136 parameters measured in the first pot.

137

138 **Leaf gas exchange and sampling of unlabelled material**

139 Leaf gas exchange measurements were conducted on plants of the unlabelled pot,
140 which had been subjected to the same N and soil water resource levels as those of the labelled
141 pot. Measurements took place on the same day as the ¹³C labelling. The following variables
142 were measured on five of the youngest fully expanded leaves after 4 h in the light:
143 transpiration rate in the light (E_i), stomatal conductance to H₂O in the light (g_s), and CO₂
144 assimilation rate (A). In addition, leaf dark respiration rate (r_i) was measured after 5 h in the
145 dark. Measurements were conducted under standardized conditions with a portable
146 photosynthesis system (Li-6400, Li-Cor Inc.), using a dew point generator (Li-610, Li-Cor
147 Inc.) and a CO₂ source to ensure constant relative humidity (60%) and CO₂ concentration
148 (400 $\mu\text{mol mol}^{-1}$) in the incoming flow of the Li-6400 leaf chamber. A 1000 $\mu\text{mol m}^{-2} \text{s}^{-1}$
149 light source (6400-02B, Li-Cor Inc.) was used for measurements in the light.

150 Leaf gas exchange measurements were performed at 1000 $\mu\text{mol m}^{-2} \text{s}^{-1}$, close to the

151 plants' maximum photosynthetic ability, to maximise the expression of physiological
152 differences among plants. Since the other environmental conditions were kept equal, A and g_s
153 at $1000 \mu\text{mol m}^{-2} \text{s}^{-1}$ are expected to be proportional to A and g_s at $400 \mu\text{mol m}^{-2} \text{s}^{-1}$ (e.g. Ye
154 and Yu, 2008) and can be related to the physiology of plants growing at $400 \mu\text{mol m}^{-2} \text{s}^{-1}$.

155 Bulk leaf and root biomass from the unlabelled pots were dried (48h at 60°C), and
156 finely ground prior to determination of C and N concentration and $\delta^{13}\text{C}$ analysis. Soil was
157 sampled as described below, and bulk soil C and N concentrations, $\delta^{13}\text{C}$ signatures as well as
158 microbial biomass $\delta^{13}\text{C}$, C and N were measured (see below).

159

160 **^{13}C labelling and measurements of $\delta^{13}\text{C}$ of respired CO_2**

161 A 15 minute ^{13}C - CO_2 pulse was applied to the plants at peak biomass (i.e., 86 days
162 old) at the end of a 10-hour dark period, to avoid mixing labelled and unlabelled recent
163 photoassimilates. Due to growth conditions of constant photoperiod and temperature, stem
164 expansion was not yet initiated in our wheat plants. Consequently, measurements were done
165 at a stage that was similar to stage 5 on the Feekes scale albeit with a higher number of leaves
166 (i.e. most of aboveground biomass consisted of leaves). Pots were labelled and measured
167 $\delta^{13}\text{C}_{\text{R-soil}}$ and $\delta^{13}\text{C}_{\text{R-shoot}}$ one after the other, over an 18-day period during which chamber
168 environmental conditions and $\delta^{13}\text{C}$ of background CO_2 were constant.

169 To avoid diffusion of labelled CO_2 into the soil and to maintain above- and
170 belowground compartments separate during subsequent gas measurements, a 1 cm-thick agar
171 gel (at 30°C , to avoid plant damage) was poured around the soil collar prior to labelling. The
172 pot containing the plants was then inserted in a custom-built transparent air-tight PVC main
173 chamber (29 cm diameter, 72 cm high), equipped with a fan to ensure good air mixing and a
174 septum for gas sampling. A custom-built 0.25 L polyethylene soil chamber was fitted air-
175 tight on the soil collar, inside the main chamber (see detailed description of setup in

176 supplementary material). The main chamber and the soil chamber were both connected
177 independently online to an IRMS via a custom-built setup, enabling measurements of $\delta^{13}\text{C}_{\text{R-}}$
178 shoot and $\delta^{13}\text{C}_{\text{R-soil}}$ every 26 minutes, and to an infra-red gas analyzer (Li-840, Li-Cor Inc.,
179 Lincoln, NE, USA), measuring CO_2 concentrations continuously. Because the agar gel
180 prohibited soil CO_2 to diffuse into the main chamber, $\delta^{13}\text{C}_{\text{R-shoot}}$ was measured directly.

181 Plant aboveground biomass was labelled by dissolving 10.48 mg of 99% pure ^{13}C -
182 Na_2CO_3 in the chamber, which amounted to $500 \mu\text{mol mol}^{-1}$ of $^{13}\text{C-CO}_2$ in the chamber
183 headspace. The labelled carbonate was placed in a cup inside the chamber, and sulphuric acid
184 was injected in excess into the cup through a septum. To ensure photosynthetic uptake of the
185 ^{13}C label, photosynthetically active radiation (PAR) of app. $400 \mu\text{mol m}^{-2} \text{s}^{-1}$ was maintained
186 inside the chamber during labelling, using a greenhouse lamp positioned outside the chamber.
187 Chamber temperature was monitored, ensuring heating of the chamber due to the lamp was
188 negligible. The effectiveness of the uptake of labelled CO_2 was controlled by monitoring CO_2
189 concentration inside the chamber. After 15 minutes, the chamber was opened and flushed
190 with outside air for five minutes. Before the online $\delta^{13}\text{C}$ measurements started, the chamber
191 was closed and flushed with CO_2 -free synthetic air until all CO_2 was removed. To avoid any
192 artefact due to potential contamination of soil efflux CO_2 by enriched $^{13}\text{C-CO}_2$ during the
193 labelling, we considered only gas measurements performed at least 2h after the pulse.

194 To avoid re-assimilation of respired label, $\delta^{13}\text{C}_{\text{R-soil}}$ and $\delta^{13}\text{C}_{\text{R-shoot}}$ were monitored
195 online in the dark for two days. Air humidity was also monitored to make sure it remained
196 stable.

197 After two days of monitoring, soil was sampled (5cm diameter core over the entire
198 pot depth), sieved (2mm mesh) and split into two subsamples. One subsample was dried (48h
199 at 60°C) and used for bulk soil analyses of $\delta^{13}\text{C}$ (see below) and total C and N concentrations
200 after manually removing the roots. The second subsample was kept at 4°C and used for

201 determination of microbial biomass $\delta^{13}\text{C}$, C and N (see below). Roots were collected by wet
202 sieving of the soil remaining in the pot after coring. Leaves were cut 1 cm above the root
203 crown. Leaf, root and soil (after removal of roots) samples were dried (60°C for 48h) and
204 finely ground prior to isotope ratio analysis (see below).

205

206 **C, N and $\delta^{13}\text{C}$ in soil microbial biomass**

207 C, $\delta^{13}\text{C}$ and N of soil microbial biomass were determined by fumigation-extraction.
208 From each sieved soil sample, an approximately 10 g subsample was fumigated for 24h with
209 chloroform vapour before extraction, while another approximately 10 g subsample was
210 extracted without fumigation. Soil was vigorously shaken for 30 minutes in a K_2SO_4
211 extraction solution (0.5M for microbial biomass, 0.03M for isotope ratio analysis). The
212 extracts were then filtered and kept frozen until total organic C and N analysis (TOC analyser
213 DIMA TOC-100, Dimatec, Essen, Germany) or lyophilized before isotope ratio analysis (see
214 below). Microbial biomass C was calculated as [(total C in fumigated soil) - (total C in non-
215 fumigated soil)] / 0.45, and microbial biomass N was calculated as [(total N in fumigated
216 soil) - (total N in non-fumigated soil)] / 0.54 (Brookes *et al.* 1985; Vance *et al.* 1987; Wu *et*
217 *al.* 1990). Microbial biomass $\delta^{13}\text{C}$ was calculated as

$$\delta^{13}\text{C}_{\text{microbes}} = \frac{\delta^{13}\text{C}_F \times C_F - \delta^{13}\text{C}_{\text{NF}} \times C_{\text{NF}}}{C_F - C_{\text{NF}}} \quad (1)$$

218 where F and NF stand for fumigated and non-fumigated soil and C for total C. Gravimetric
219 soil water content was determined by comparing the mass of 10 g of soil before and after
220 drying at 105°C.

221

222 **Isotope ratio mass spectrometry measurements**

223 The $\delta^{13}\text{C}$ value of gas samples was measured with a modified Gasbench II periphery
224 (Finnigan MAT, Bremen, Germany) equipped with a custom-built cold trap coupled to the

225 IRMS (Delta^{plus}XP, Finnigan MAT). The $\delta^{13}\text{C}$ values in bulk leaf, root and soil as well as in
 226 microbial biomass extracts were measured with an elemental analyser (Flash EA 1112 Series,
 227 Thermo Italy, Rhodano, Italy) coupled to an IRMS (Delta^{plus}XP). The long-term precision (~
 228 1.5 years) of the quality control standard (caffeine) was 0.09‰ for $\delta^{13}\text{C}$. Isotopic values are
 229 expressed in delta notation (‰), as the sample isotope ratio R_{sample} ($^{13}\text{C}/^{12}\text{C}$) relative to that of

230 the international standard R_{standard} (Vienna Pee Dee Belemnite, V-PDB):
$$\delta = \frac{R_{\text{sample}}}{R_{\text{standard}}} - 1$$

231 $\delta^{13}\text{C}$ values were expressed as atom% to estimate the total amount of ^{13}C added by
 232 pulse-labelling as follows:

$$\text{atom}\% = \frac{0.0111802 \times \left(\frac{\delta^{13}\text{C}}{1000} + 1 \right)}{1 + 0.0111802 \times \left(\frac{\delta^{13}\text{C}}{1000} + 1 \right)} \quad (2)$$

233 where 0.0111802 is the standard value for the C isotope ratio of V-PDB.

234 Excess ^{13}C was calculated in plant, soil CO_2 efflux and soil microbial biomass to take
 235 into account differences in plant biomass between resource levels and consequently the
 236 possible differences in assimilation of labelled C during the $^{13}\text{C}\text{-CO}_2$ pulse. Excess ^{13}C in the
 237 plant (either excess $^{13}\text{C}_{\text{root}}$ or excess $^{13}\text{C}_{\text{shoot}}$, depending on the tissue considered) was
 238 calculated as follows:

$$\text{excess } ^{13}\text{C}_{\text{plant}} = (\text{atom}\%_s - \text{atom}\%_b) \times B \times \frac{\text{C}\%}{100} \times \frac{1}{M_C} \quad (3)$$

239 where $\text{atom}\%_s$ and $\text{atom}\%_b$ are sample and background (measured on the unlabelled sample)
 240 $\text{atom}\%$ of the plant tissue, respectively. B is the dry mass (mg m^{-2}), C% is C concentration
 241 and M_C is the molar mass of carbon (12 g mol^{-1}).

242 Excess $^{13}\text{C}_R$ in shoot-respired CO_2 (excess $^{13}\text{C}_{R\text{-shoot}}$) or soil CO_2 efflux (excess $^{13}\text{C}_{R\text{-soil}}$)
 243 was calculated as:

$$\text{excess } ^{13}\text{C}_R = (\text{atom}\%_s - \text{atom}\%_b) \times F \quad (4)$$

244 where F is either shoot respiration rate or soil CO₂ efflux rate (mmol m⁻² h⁻¹). Soil CO₂ efflux
 245 rate is expressed relative to soil surface area.

246 Excess ¹³C in soil microbial biomass (excess ¹³C_{microbes}) was calculated as follows:

$$\text{excess } ^{13}\text{C}_{\text{microbes}} = (\text{atom}\%_s - \text{atom}\%_b) \times \frac{\text{TOC}}{M_C} \quad (5)$$

247 where TOC is the total organic C content of microbial biomass (μg g⁻¹ dry soil). Since
 248 measurements of the natural background δ¹³C of soil microbial biomass were not available,
 249 we used the background δ¹³C of root biomass as a proxy for atom%_b of soil microbial C.

250 The total amount of label released in soil CO₂ efflux was calculated by integrating
 251 excess ¹³C_{R-soil} released during the measurement period (from 2 to 48h after the pulse). Since
 252 none of the standard regression models (linear, polynomial with a reasonable degree,
 253 exponential, etc.) fitted the excess ¹³C_{R-soil} curve, we integrated it numerically using 3-point
 254 quadratic interpolation. Note that due to IRMS failure, the gas measurements of pot 6 stopped
 255 24 hours after labelling (i.e., 5 hours after peaking). Excess ¹³C_{R-soil} values after that time
 256 were predicted with an exponential decay function that was fitted to the data available for that
 257 pot between 19 hours (the time of maximum excess ¹³C_{R-soil}) and 24 hours (IRMS failure)
 258 after labelling.

259

260 **Statistical analyses**

261 Data were analysed using R 2.14.2 (R Development Core Team 2012). The
 262 experimental setup was not intended to test the effects of different resource levels, but to
 263 identify functional relationships between the isotopic signatures and the ecophysiological
 264 variables measured over a set of plants that differed in their physiology. We used the
 265 following parameters to characterize changes in excess ¹³C_{R-shoot} and excess ¹³C_{R-soil} over

266 time: i) initial slope of decreasing excess $^{13}\text{C}_{\text{R-shoot}}$, ii) time between labelling and maximum
267 excess $^{13}\text{C}_{\text{R-soil}}$, iii) maximum excess $^{13}\text{C}_{\text{R-soil}}$, iv) total excess $^{13}\text{C}_{\text{R-soil}}$ (i.e. its curve area),
268 which provided a more integrative estimate of total amount of label released during the
269 measurement period. The following exponential decay function was used to estimate mean
270 residence time and half-life of the ^{13}C label in shoots:

$$N(t) = N_0 e(-\lambda t) \quad (6)$$

271 where t is the time after labelling, N_0 the initial excess $^{13}\text{C}_{\text{R-shoot}}$, λ the decay constant and $N(t)$
272 the excess $^{13}\text{C}_{\text{R-shoot}}$ at time t . Mean residence time (τ) of ^{13}C in shoot-respired CO_2 was then
273 calculated as $[\tau = 1/\lambda]$, and half-life of ^{13}C label in shoots as $[t_{1/2} = \ln(2)/\lambda = \tau \ln(2)]$.

274 Relationships between these excess $^{13}\text{C}_{\text{R}}$ variables and leaf gas exchange
275 measurements were tested using linear regression models with all six plants.

276

277 **Results**

278 **Physiologically different plants**

279 The different combinations of resource levels of N and soil water resulted in the
280 sought-after wide range of plant physiological characteristics, providing the set of plants
281 necessary for our ^{13}C pulse-chase experiment. Leaf dark respiration rate (r_1) varied by 1000%
282 (Table 1), root:shoot ratios by 850%, transpiration rate in the light (E_l) varied by about 300%,
283 stomatal conductance to H_2O in the light (g_s) varied by about 240%, while CO_2 assimilation
284 rate (A) and intrastomatal : atmospheric partial pressure of CO_2 (c_i/c_a) varied by about 25%. It
285 is to be noted that due to a Li6400 block temperature control malfunction, although E_l and g_s
286 are significantly positively correlated, they are not on a 1:1 relation across plants ($R^2=0.72$,
287 $p=0.033$).

288 The differences in physiology due to N and soil water resource levels were reflected
289 in plant C and N concentrations as well as their $\delta^{13}\text{C}$ values (Table 1). Leaf, root and soil N

290 concentrations varied between 2.3 and 7.2%, 1.2 and 3.4% and 0.4 to 0.8%, respectively.
291 Prior to ^{13}C labelling, the $\delta^{13}\text{C}$ values of leaves and roots were on average $-27.83\pm 0.54\%$ and
292 $-27.46\pm 0.42\%$, respectively (overall mean \pm SE), and the $\delta^{13}\text{C}$ value of bulk soil was on
293 average $-25.33\pm 0.10\%$.

294 After labelling, leaf excess ^{13}C showed a 2.4-fold range, while root excess ^{13}C showed
295 a 10-fold range (Table 2). Soil showed little to no labelling, while excess ^{13}C in soil microbial
296 biomass showed a 4.666-fold range (Table 2).

297

298 **Excess ^{13}C of shoot- and soil-respired CO_2**

299 Pulse-labelling triggered a large initial excess $^{13}\text{C}_{\text{R-shoot}}$ of up to $11 \mu\text{mol m}^{-2} \text{h}^{-1}$, 2h
300 after labelling (Fig. 1a). $t_{1/2}$ ranged from 7.2 to 14.5 hours, and τ ranged from 10.4 to 20.9
301 hours (Table 2). Excess $^{13}\text{C}_{\text{R-shoot}}$ decreased continuously during the following two days,
302 however, showing different temporal patterns for the six wheat plants studied. In contrast,
303 excess $^{13}\text{C}_{\text{R-soil}}$ values first increased for all plants, and then peaked between the 15th and the
304 21st hour after labelling (Fig. 1b). At the end of the measurement period, excess $^{13}\text{C}_{\text{R-soil}}$ was
305 still positive ($0.85\pm 0.33 \mu\text{mol m}^{-2} \text{h}^{-1}$ across all six plants).

306

307 **Relationships between excess ^{13}C and physiological variables**

308 The initial slope of decreasing excess $^{13}\text{C}_{\text{R-shoot}}$ with time, a proxy for rate of C
309 transfer belowground (see Discussion), was significantly negatively related to leaf stomatal
310 conductance (Fig. 2a, $R^2=0.72$, $p=0.033$) across all plants. None of the other ecophysiological
311 variables was significantly related with the initial slope of decreasing excess $^{13}\text{C}_{\text{R-shoot}}$,
312 although the relationship with E_l ($R^2=0.50$, $p=0.12$) tended to be stronger than with A
313 ($R^2=0.24$, $p=0.32$) or c_i/c_a ($R^2=0.18$, $p=0.40$). Both τ and $t_{1/2}$ were negatively related to r_1
314 ($R^2=0.81$, $p=0.014$), as a higher respiration rate lead to faster loss of labelled C.

315 The time until maximum excess $^{13}\text{C}_{\text{R-soil}}$ values were reached, i.e., the transfer time,
316 decreased significantly with stomatal conductance (Fig. 2b; $R^2=0.76$, $p=0.023$). Although
317 none of the other variables showed a significant relationship with transfer time, again, the
318 relationship with E_l ($R^2=0.49$, $p=0.12$) tended to be stronger than that with A ($R^2=0.08$,
319 $p=0.60$). We found no further significant relations between excess $^{13}\text{C}_{\text{R-soil}}$ and any other soil
320 or plant variable.

321 Maximum excess $^{13}\text{C}_{\text{R-soil}}$ was negatively related to pre-labelling root $\delta^{13}\text{C}$ value
322 ($R^2=0.91$, $p=0.012$) and soil N concentration ($R^2=0.67$, $p=0.045$, Fig.3a) and positively
323 related to root excess ^{13}C after labelling ($R^2=0.80$, $p=0.039$, Fig. 4a). In addition, maximum
324 excess $^{13}\text{C}_{\text{R-soil}}$ tended to be negatively related to root N concentrations ($R^2=0.65$, $p=0.052$,
325 Fig. 3b) and leaf N concentrations ($R^2=0.62$, $p=0.064$). The total amount of label released
326 during the measurement period by soil CO_2 efflux (Fig. 1b) was positively related maximum
327 excess $^{13}\text{C}_{\text{R-soil}}$ ($R^2=0.99$, $p<0.001$) and to root excess ^{13}C after labelling ($R^2=0.85$, $p=0.025$,
328 Fig.4b), but negatively related to soil N concentrations ($R^2=0.73$, $p=0.030$, Fig.3c) and pre-
329 labelling root $\delta^{13}\text{C}$ values ($R^2=0.85$, $p=0.027$). In addition, the total amount of label released
330 tended to be positively related to leaf C concentrations ($R^2=0.55$, $p=0.091$), and negatively
331 related to leaf $\delta^{13}\text{C}$ values before labelling ($R^2=0.61$, $p=0.068$), root N concentrations
332 ($R^2=0.64$, $p=0.055$, Fig. 3d) and leaf N concentrations ($R^2=0.64$, $p=0.057$). Soil water content
333 was not significantly related to excess $^{13}\text{C}_{\text{R-shoot}}$ and excess $^{13}\text{C}_{\text{R-soil}}$ parameters (data not
334 shown).

335

336 **Discussion**

337

338 **Physiological drivers of isotopic time lags**

339 The wide range of growth conditions yielded wheat plants that covered a wide

340 physiological status range. We found a strong relationship between plant physiological status,
341 and the velocity of newly-assimilated C transfer from leaves to sink organs. In particular, the
342 controls of C transfer appear to strongly involve g_s : the larger g_s , the shorter the time between
343 assimilation and respiration of labelled C. Our plants had not yet produced stems, and their
344 leaves were of similar length, consequently the entire aboveground biomass was
345 photosynthetically active and the distance from above- to belowground was similar for all
346 plants and differences in C transport velocity depended on the time of transport, not on the
347 distance. Thus, larger g_s was associated with faster C transfer from assimilation sites to
348 respiration sites. Under growth conditions of constant day-to-day environmental parameters
349 for all plants (i.e. humidity, temperature and CO₂ concentration, as was the case in our
350 experiment), differences in plant physiology arise from differences in the plant's internal C
351 and water balance (e.g. Goldschmidt and Huber 1992; Paul and Foyer 2001; McCormick *et*
352 *al.* 2009).

353 Our results do not point towards source strength controlling C transport velocity.
354 Assimilation rate could be used as a proxy for source strength in this experiment, since the
355 plants had been kept in the dark for 10h prior to labelling, thus sucrose concentration in the
356 leaves must have been low in all plants and unlikely to modify source strength in this
357 experiment. We found no significant relationship between assimilation rate and transfer
358 velocity of labelled C, suggesting that even if source strength had a gross effect, it was
359 accompanied by other factors, resulting in no detectable net effect. In contrast, sink strength
360 controls over C transport velocity, and involving g_s , is supported by several lines of evidence.

361 First, previous experiments have established a link between g_s and C sinks: the
362 strength of C sinks is involved in controlling stomatal conductance (e.g. Koller and Thorne
363 1978; Peet and Kramer 1980; Goldschmidt and Huber 1992), together with environmental
364 conditions in the atmosphere surrounding the leaves (Lambers *et al.* 1998). In addition, sink

365 strength rather than by source strength likely drives whole-plant C allocation (Ho 1988; Paul
366 and Foyer 2001), turnover and allocation of different C pools being driven by competing C
367 sinks (Kozlowski 1992).

368 Second, shorter transfer times of newly assimilated C driven by increased sink
369 strength are consistent with the Munch hypothesis that C transport in phloem is driven by a
370 hydrostatic pressure gradient from source to sink (Gould *et al.* 2005).

371

372 In addition to transfer towards C sinks, the fate of recently assimilated C during the
373 dark period can include C storage as well as its direct respiration by aboveground biomass,
374 both of which are unlikely to represent a significant fraction of the labelled C in our
375 experiment. Storage could interfere with our interpretation of excess $^{13}\text{C}_{\text{R-soil}}$ by creating a
376 pool of labelled C that would not appear in belowground respiration. However, experimental
377 C starvation has been shown to lead to preferential allocation of recent photoassimilates
378 towards growth and respiration rather than towards starch synthesis (for example, less than
379 10% of the photoassimilates were allocated to starch synthesis in starved French bean plants
380 starved for three days, Nogues *et al.* 2004). The decrease in newly assimilated C availability
381 for aboveground respiration over time is represented by the initial slope of $^{13}\text{C}_{\text{R-shoot}}$ with
382 time, and can result from respiration by aboveground biomass, storage (but see above) or
383 transfer to sink organs. Note that it cannot be due to isotopic dilution by photosynthesis, since
384 plants were maintained in the dark. Our data show that the initial slope of $^{13}\text{C}_{\text{R-shoot}}$ is not
385 significantly related to leaf respiration rate. Therefore, we consider that in our experiment, the
386 transfer of labelled C belowground is the main driver of the initial slope $^{13}\text{C}_{\text{R-shoot}}$ with time,
387 and therefore of its observed relationship with g_s .

388 The effect of C starvation resulting from extended exposure to darkness on C storage
389 is less clear belowground than aboveground and appears to depend on plant adaptation. In

390 crop species, C starvation under prolonged darkness leads to the exhaustion of root non-
391 structural C pools fairly rapidly: within 48h in maize (Brouquisse *et al.* 1998), but more than
392 three days in French bean (Bathellier *et al.* 2009). In contrast, shading a mountain grassland
393 had no effect on starch formation in roots, which was likely related to adaptation to a short
394 growing season and to grazing (Bahn *et al.* 2013). Since wheat has been selected to maximise
395 grain production, it is expected to exhibit a crop species type of response to prolonged
396 darkness, with little storage in the dark. Thus, we hypothesize that storage of labelled C likely
397 occurred shortly after the pulse, but that it was not maintained over an extended period of
398 darkness, and only minimally interfered with the interpretation of excess $^{13}\text{C}_{\text{R-soil}}$.

399 Excess $^{13}\text{C}_{\text{R-soil}}$ responded not only to leaf gas exchange variables, but also to N
400 resources, as less label was transferred belowground under conditions of higher soil N
401 availability. We found negative relationships between N concentrations in the soil and in plant
402 tissues on the one hand, and maximum excess $^{13}\text{C}_{\text{R-soil}}$ as well as total excess $^{13}\text{C}_{\text{R-soil}}$ on the
403 other hand. These results bring further support to the sink strength hypothesis, for several
404 reasons. Firstly, N fertilization generally decreases plant root:shoot ratio (Mooney *et al.* 1995;
405 Lehmeier *et al.* 2008), resulting in a relatively smaller plant belowground biomass C sink for
406 root growth and maintenance (Amthor 2000). Secondly, higher N availability reduces the C
407 costs associated with N assimilation, which represent a large fraction of root respiration
408 (Bloom *et al.* 1992).

409

410 **Identity of respired carbon pools**

411 Plant physiological drivers seem to control rate of C transfer belowground, i.e., two of
412 the three main components of isotopic time lags: transfer velocity and quantity of C
413 transferred. Our experimental design did not allow identifying the third component of
414 isotopic time lag, the identity of labelled molecules transported and respired. Nonetheless, we

415 can hypothesise what has been transferred based on the consistent, albeit variable in its
416 magnitude, three-phase pattern of temporal dynamics of excess $^{13}\text{C}_{\text{R-shoot}}$ and $^{13}\text{C}_{\text{R-soil}}$,
417 observed along the wide physiological status range created with the six plants: 1) during the
418 first 10h, excess $^{13}\text{C}_{\text{R-shoot}}$ strongly decreased while excess $^{13}\text{C}_{\text{R-soil}}$ increased, 2) from the 10th
419 to the 25th hours, excess $^{13}\text{C}_{\text{R-shoot}}$ decreased while excess $^{13}\text{C}_{\text{R-soil}}$ peaked, 3) after the 25th
420 hour, both excess $^{13}\text{C}_{\text{R-shoot}}$ and $^{13}\text{C}_{\text{R-soil}}$ decreased at a slower rate. These results are consistent
421 with previous studies that showed the presence of several C pools with different turnover
422 times (Schnyder *et al.* 2003; Carbone and Trumbore 2007; Lehmeier *et al.* 2008; Lehmeier *et*
423 *al.* 2010). The identity of the different C pools has not been characterised in our study.
424 However, specific C pools that differed in their turnover times have been identified in *Lolium*
425 *perenne* grown under controlled conditions (Schnyder *et al.* 2003; Lehmeier *et al.* 2008;
426 Lehmeier *et al.* 2010) as well as in perennial grasses and shrubs (Carbone and Trumbore
427 2007). Based on these experiments, we hypothesize that the first phase can probably be
428 attributed to a fast-turnover C pool, perhaps organic acids (Lehmeier *et al.* 2010). In the
429 second phase, a second C pool, possibly mono- or disaccharides such as sucrose might have
430 been respired (Scofield *et al.* 2009; Lehmeier *et al.* 2010). Finally, the third phase could result
431 from the respiration of storage compounds such as fructans or transitory starch (Scofield *et*
432 *al.* 2009; Lehmeier *et al.* 2010).

433 Experimental conditions of prolonged darkness after labelling may have induced
434 changes in the identity of the substrates fuelling respiration, since for example leaves kept in
435 the dark switch respiratory substrate from carbohydrates to fatty acids, upon depletion of the
436 former (Tcherkez *et al.* 2003). However, we measured consistently positive excess $^{13}\text{C}_{\text{R}}$
437 throughout our experiment, indicating that respiration was still at least partially fuelled by C
438 fixed during labelling. Thus, despite the long darkness exposure which might have triggered
439 the use of older C pools stored in plant tissues before labelling (Nogues *et al.* 2004), our

440 results are consistent with the hypothesis of three recently assimilated C pools fuelling the
441 three-phase pattern of temporal dynamics of excess $^{13}\text{C}_{\text{R-shoot}}$ and $^{13}\text{C}_{\text{R-soil}}$.

442

443 **Isotopic time lag and water status**

444 Based on the Münch hypothesis, which implies a tight connection between water and
445 C fluxes in plants, we were expecting that transpiration would impact the isotopic time lag.
446 Although not significant (but see result section), our results suggest that higher transpiration
447 tended to be associated with higher phloem flux rate, i.e., a shorter transfer times and thus
448 shorter time lags between assimilation and respiration of labelled C. These results are in
449 contrast with some modelling studies which have suggested that higher transpiration,
450 especially at the diurnal scale, should be associated with a decrease in phloem flux rate, due
451 to the increase of phloem viscosity resulting from higher water loss and decreased water
452 transfer from xylem to phloem (Hölttä *et al.* 2005; Lacoite and Minchin 2008). This
453 discrepancy could arise from three non-exclusive hypotheses. First, differences in hydraulic
454 conductance among plants could modify the relation between E_i , g_s and phloem viscosity
455 across plants. Indeed, transpiration rate is a function of i) the water potential gradient between
456 soil and atmosphere around the plant, and ii) plant hydraulic conductance. In our experiment,
457 the water potential gradient does not appear to play a major role in explaining excess $^{13}\text{C}_{\text{R}}$
458 patterns, since relative humidity was kept constant and equal among the different plants, and
459 changes in excess $^{13}\text{C}_{\text{R}}$ were not related to soil water content. In contrast, hydraulic
460 conductance may have differed among plants along the physiological status range, as plant N
461 availability could affect root hydraulic conductance (Ruggiero and Angelino, 2007). Second,
462 changes in the velocity of C transfer from assimilation to respiration should be considered as
463 the net effect of changes in phloem velocity and concentration, due to changes in water
464 availability and to changes in hydrostatic pressure related to source and sink activities. On

465 one hand, higher E_l and g_s can be associated with lower leaf water potential, therefore
466 requiring more sugar loading in the phloem to maintain turgor and drive the pressure flow.
467 Combined higher sugar concentration in the sieve tubes and lower water content result in
468 higher phloem viscosity, decreasing phloem velocity, but the sap is more concentrated in C.
469 On the other hand, changes in sink strength could also alter phloem velocity by modifying the
470 hydrostatic pressure difference in the phloem and thus phloem velocity.. Third, under steady-
471 state conditions, g_s and consequently E_l are plant-regulated, based on the amount of soil water
472 available (Lambers *et al.* 1998). In that case, higher water availability relative to the plant
473 needs would be associated with higher g_s , higher E_l and higher water diffusion from xylem to
474 phloem near the phloem loading sites, resulting in a decreased phloem viscosity and
475 associated increased sap velocity. This third hypothesis would be consistent with previous
476 studies that showed decreased C transfer velocity under drought (Ruehr *et al.* 2009;
477 Brüggemann *et al.* 2011 and references therein). In the absence of day-to-day environmental
478 variations, control by transpiration and thus stomatal conductance over C transfer from
479 assimilation to respiration is likely released due to plant adaptation to constant water supply
480 and loss. Consequently, although we found no strong evidence (p values around 0.1, but see
481 result section) for transpiration being a prominent driver of the isotopic time lag under our
482 experimental conditions, much in contrast to stomatal conductance, plant water loss is likely
483 to play an important role, especially under field conditions.

484

485 In conclusion, based on leaf gas exchange and excess $^{13}\text{C}_R$ measurements, our study
486 suggests that under controlled conditions, C sink strength is the main driver of the amount
487 and velocity of recently assimilated C allocated belowground. Our results show that, in
488 addition to known effects of environmental conditions, plant physiological status contributes
489 to shaping the isotopic time lag between assimilation and respiration.

490

491 **Acknowledgments**

492 We thank G r me Tokpa for his help with gas exchange measurements, Annika Lenz
493 for help with isotope measurements, Roland A. Werner for helpful comments on the
494 manuscript. YS was supported by the Swiss National Science Foundation (project n 3100A0-
495 105273/1).

496

497 **References**

498

499 Amthor, JS (2000) The McCree-de Wit-Penning de Vries-Thornley respiration paradigms: 30
500 years later. *Annals of Botany* **86**, 1-20.

501 Bahn, M, Lattanzi, FA, Hasibeder, R, Wild, B, Koranda, M, Danese, V, Brueggemann, N,
502 Schmitt, M, Siegwolf, R, Richter, A (2013) Responses of belowground carbon
503 allocation dynamics to extended shading in mountain grassland. *New Phytologist* **198**,
504 116–126.

505 Bathellier, C, Tcherkez, G, Mauve, C, Bligny, R, Gout, E, Ghashghaie, J (2009) On the
506 resilience of nitrogen assimilation by intact roots under starvation, as revealed by
507 isotopic and metabolomic techniques. *Rapid Communications in Mass Spectrometry*
508 **23**, 2847–2856.

509 Bloom, AJ, Sukrapanna, SS, Warner, RL (1992) Root respiration associated with ammonium
510 and nitrate absorption and assimilation by barley. *Plant Physiology* **99**, 1294-1301.

511 Brookes, PC, Landman, A, Pruden, G, Jenkinson, DS (1985) Chloroform fumigation and the
512 release of soil nitrogen - a rapid direct extraction method to measure microbial
513 biomass nitrogen in soil. *Soil Biology & Biochemistry* **17**, 837-842.

514 Brouquisse, R, Gaudillere, JP, Raymond, P (1998) Induction of a carbon-starvation-related

515 proteolysis in whole maize plants submitted to light/dark cycles and to extended
516 darkness. *Plant Physiology* **117**, 1281–1291.

517 Brüggemann, N, Gessler, A, Kayler, Z, Keel, SG, Badeck, F, Barthel, M, Boeckx, P,
518 Buchmann, N, Brugnoli, E, Esperschütz, J, Gavrichkova, O, Ghashghaie, J, Gomez-
519 Casanovas, N, Keitel, C, Knohl, A, Kuptz, D, Palacio, S, Salmon, Y, Uchida, Y, Bahn,
520 M (2011) Carbon allocation and carbon isotope fluxes in the plant-soil-atmosphere
521 continuum: a review. *Biogeosciences* **8**, 3457-3489.

522 Buchmann, N, Brooks, JR, Rapp, KD, Ehleringer, JR (1996) Carbon isotope composition of
523 C₄ grasses is influenced by light and water supply. *Plant, Cell & Environment* **19**,
524 392-402.

525 Carbone, MS, Trumbore, SE (2007) Contribution of new photosynthetic assimilates to
526 respiration by perennial grasses and shrubs: residence times and allocation patterns.
527 *New Phytologist* **176**, 124-135.

528 Dawson, TE, Mambelli, S, Plamboeck, AH, Templer, PH, Tu, KP (2002) Stable isotopes in
529 plant ecology. *Annual Review of Ecology, Evolution and Systematics* **33**, 507-559.

530 Epron, D, Bahn, M, Derrien, D, Lattanzi, FA, Pumpanen, J, Gessler, A, Hogberg, P, Maillard,
531 P, Dannoura, M, Gerant, D, Buchmann, N (2012) Pulse-labelling trees to study carbon
532 allocation dynamics: a review of methods, current knowledge and future prospects.
533 *Tree Physiology* **32**, 776-798.

534 Evans, JR, Sharkey, TD, Berry, JA, Farquhar, GD (1986) Carbon isotope discrimination
535 measured concurrently with gas-exchange to investigate CO₂ diffusion in leaves of
536 higher-plants. *Australian Journal of Plant Physiology* **13**, 281-292.

537 Farquhar, GD, Ehleringer, JR, Hubick, KT (1989) Carbon isotope discrimination and
538 photosynthesis. *Annual Review of Plant Physiology and Plant Molecular Biology* **40**,
539 503-537.

540 Gessler, A, Tcherkez, G, Peuke, AD, Ghashghaie, J, Farquhar, GD (2008) Experimental
541 evidence for diel variations of the carbon isotope composition in leaf, stem and
542 phloem sap organic matter in *Ricinus communis*. *Plant, Cell & Environment* **31**, 941-
543 953.

544 Goldschmidt, EE, Huber, SC (1992) Regulation of photosynthesis by end-product
545 accumulation in leaves of plants storing starch, sucrose, and hexose sugars. *Plant*
546 *Physiology* **99**, 1443-1448.

547 Gould, N, Thorpe, MR, Koroleva, O, Minchin , PEH (2005) Phloem hydrostatic pressure
548 relates to solute loading rate: a direct test of the Münch hypothesis. *Functional Plant*
549 *Biology* **32**, 1019-1026. Ho, LC (1988) Metabolism and compartmentation of imported
550 sugars in sink organs in relation to sink strength. *Annual Review of Plant Physiology*
551 *and Plant Molecular Biology* **39**, 355-378.

552 Hölttä, T, Vesala, T, Sevanto, S, Perämäki, M, Nikinmaa, E (2005) Modeling xylem and
553 phloem water flows in trees according to cohesion theory and Münch hypothesis.
554 *Trees* **20**, 67-78.

555 Kodama, N, Barnard, RL, Salmon, Y, Weston, C, Ferrio, JP, Holst, J, Werner, RA, Saurer, M,
556 Rennenberg, H, Buchmann, N, Gessler, A (2008) Temporal dynamics of the carbon
557 isotope composition in a *Pinus sylvestris* stand: from newly assimilated organic
558 carbon to respired carbon dioxide *Oecologia* **156**, 737-750.

559 Koller, HR, Thorne, JH (1978) Soybean pod removal alters leaf diffusion resistance and
560 leaflet orientation. *Crop Science* **18**, 305-307.

561 Kozlowski, TT (1992) Carbohydrate sources and sinks in woody plants. *Botanical Review* **58**,
562 107-222.

563 Kuzyakov, Y, Gavrichkova, O (2010) Time lag between photosynthesis and carbon dioxide
564 efflux from soil: a review of mechanisms and controls. *Global Change Biology* **16**,

565 3386-3406.

566 Lacointe, A, Minchin, PEH (2008) Modelling phloem and xylem transport within a complex
567 architecture. *Functional Plant Biology* **35**, 772-780.

568 Lambers, H, Chapin, FS, Pons, T (1998) Plant physiological ecology. In 'Plant physiological
569 ecology.' pp. 185-189. (Springer New York, USA)

570 Lehmeier, CA, Lattanzi, FA, Schäufele, R, Schnyder, H (2010) Nitrogen deficiency increases
571 the residence time of respiratory carbon in the respiratory substrate supply system of
572 perennial ryegrass. *Plant, Cell & Environment* **33**, 76-87.

573 Lehmeier, CA, Lattanzi, FA, Schäufele, R, Wild, M, Schnyder, H (2008) Root and shoot
574 respiration of perennial ryegrass are supplied by the same substrate pools - assessment
575 by dynamic ¹³C labeling and compartmental analysis of tracer. *Plant Physiology* **148**,
576 1148-1158.

577 Litton, CM, Raich, JW, Ryan, MG (2007) Carbon allocation in forest ecosystems. *Global
578 Change Biology* **13**, 2089-2109.

579 McCormick, AJ, Watt, DA, Cramer, MD (2009) Supply and demand: sink regulation of sugar
580 accumulation in sugarcane. *Journal of Experimental Botany* **60**, 357-364.

581 Mencuccini, M, Hölttä, T (2010) The significance of phloem transport for the speed with
582 which canopy photosynthesis and belowground respiration are linked. *New
583 Phytologist* **185**, 189-203.

584 Mooney, H, Fichtner, K, Schulze, E (1995) Growth, photosynthesis and storage of
585 carbohydrates and nitrogen in *Phaseolus-lunatus* in relation to resource availability.
586 *Oecologia* **104**, 17-23.

587 Nogués, S, Tcherkez, G, Cornic, G, Ghashghaie, J (2004) Respiratory carbon metabolism
588 following illumination in intact french bean leaves using ¹³C/¹²C isotope labeling.
589 *Plant Physiology* **136**, 3245-3254.

590 Paul, MJ, Foyer, CH (2001) Sink regulation of photosynthesis. *Journal of Experimental*
591 *Botany* **52**, 1383-1400.

592 Peet, MM, Kramer, PJ (1980) Effects of decreasing source-sink ratio in soybeans on
593 photosynthesis, photo-respiration, transpiration and yield. *Plant, Cell & Environment*
594 **3**, 201-206.

595 Poorter, H, Nagel, O (2000) The role of biomass allocation in the growth response of plants
596 to different levels of light, CO₂, nutrients and water: a quantitative review. *Australian*
597 *Journal of Plant Physiology* **27**, 595-607.

598 R Development Core Team (2012) 'R: A language and environment for statistical computing.'
599 (R Foundation for Statistical Computing: Vienna, Austria)

600 Ruehr, NK, Offermann, CA, Gessler, A, Winkler, JB, Ferrio, JP, Buchmann, N, Barnard, RL
601 (2009) Drought effects on allocation of recent carbon: from beech leaves to soil CO₂
602 efflux. *New Phytologist* **184**, 950-961.

603 Ruggiero, C, Angelino, G (2007) Changes of root hydraulic conductivity and root/shoot ratio
604 of durum wheat and barley in relation to nitrogen availability and mercury exposure.
605 *Italian Journal of Agronomy* **2**, 281-290.

606 Schnyder, H, Schäufele, R, Lötscher, M, Gebbing, T (2003) Disentangling CO₂ fluxes: direct
607 measurements of mesocosm-scale natural abundance ¹³CO₂/¹²CO₂ gas exchange, ¹³C
608 discrimination, and labelling of CO₂ exchange flux components in controlled
609 environments. *Plant, Cell & Environment* **26**, 1863-1874.

610 Scofield, GN, Ruuska, SA, Aoki, N, Lewis, DC, Tabe, LM, Jenkins, CLD (2009) Starch
611 storage in the stems of wheat plants: localization and temporal changes. *Annals of*
612 *Botany* **103**, 859-868.

613 Tcherkez, G, Nogués, S, Bleton, J, Cornic, G, Badeck, F, Ghashghaie, J (2003) Metabolic
614 origin of carbon isotope composition of leaf dark-respired CO₂ in french bean. *Plant*

615 *Physiology* **131**, 237-244.

616 Van Bel, AJE (2003) The phloem, a miracle of ingenuity. *Plant, Cell & Environment* **26**, 125-

617 149.

618 Vance, ED, Brookes, PC, Jenkinson, DS (1987) An extraction method for measuring soil

619 microbial biomass C. *Soil Biology Biochemistry* **19**, 703-707.

620 Werner, C, Gessler, A (2011) Diel variations in the carbon isotope composition of respired

621 CO₂ and associated carbon sources: a review of dynamics and mechanisms.

622 *Biogeosciences* **8**, 2437-2459.

623 Wu, J, Joergensen, RG, Pommerening, B, Chaussod, R, Brookes, PC (1990) Measurement of

624 soil microbial biomass C by fumigation extraction - an automated procedure. *Soil*

625 *Biology & Biochemistry* **22**, 1167-1169.

626 Ye, ZP, Yu, Q (2008) A coupled model of stomatal conductance and photosynthesis for winter

627 wheat. *Photosynthetica* **46**, 637-640.

628

629 **Table 1:** Physiological range of wheat plants with their resources level: soil water content (SWC) and fertilization, including root:shoot ratio and
 630 the following leaf gas exchange parameters: CO₂ assimilation rate (A), Stomatal conductance to H₂O in the light (g_s), transpiration rate in the
 631 light (E_l), dark respiration (r_l), and intrastomatal:atmospheric partial pressure of CO₂ (c_i/c_a), as well as pre-labelling δ¹³C in bulk leaves, roots,
 632 soil as well as C and N concentrations in bulk leaves, roots, soil and soil microbial biomass. na indicates unavailable data.

Plant	SWC (%)	fertilization	Root:shoot ratio	A	g _s	E _l	r _l	c _i /c _a	Bulk leaves			Bulk roots			Bulk soil			Soil microbial biomass	
				(μmol m ⁻² s ⁻¹)	(mol H ₂ O m ⁻² s ⁻¹)	(mmol m ⁻² s ⁻¹)	(μmol m ⁻² s ⁻¹)	δ ¹³ C (‰)	C (%)	N (%)	δ ¹³ C (‰)	C (%)	N (%)	δ ¹³ C (‰)	C (%)	N (%)	C (%)	N (%)	
1	47	No	2.02	16.5	0.35	3.45	0.46	0.76	-29	40.8	3.3	-28.7	51.9	1.2	-25.6	10.8	0.4	49.4	0.18
2	63	No	1.43	15.26	0.57	4.23	0.08	0.85	-29.3	41	2.8	-27.9	49.9	1.2	-25.3	12.1	0.5	39.1	0.1
3	71	No	3.66	12.72	0.33	2.35	0.1	0.81	-28.4	41.7	2.3	na	na	na	-24.9	12.2	0.5	44.5	0.1
4	47	Yes	0.43	16.46	0.24	1.53	0.74	0.68	-25.8	39	7.2	-26.2	50.4	2.7	-25.4	8.7	0.8	38.9	13.6
5	63	Yes	0.64	20.48	0.44	2.71	0.82	0.76	-26.9	39.5	6.2	-26.7	47.8	3.4	-25.4	9.9	0.8	45.1	5.5
6	71	Yes	0.74	20.48	0.4	2.7	0.45	0.74	-27.5	39.3	5.4	-28	45.1	1.6	-25.6	11.5	0.8	31.1	1.4

633

634 **Table 2:** Post-labelling excess ^{13}C in leaf biomass, root biomass, bulk soil and microbial
 635 biomass, as well as mean residence time of ^{13}C label in shoots (τ) and half-life ($t_{1/2}$) of ^{13}C in
 636 shoot-respired CO_2 . na indicates unavailable data.

plant	Excess ^{13}C				τ (h)	$t_{1/2}$ (h)
	leaves	roots	soil	soil microbial biomass		
	($\mu\text{mol m}^{-2}$ dry leaf)	($\mu\text{mol m}^{-2}$ dry root)	($\mu\text{mol g}^{-1}$ dry soil)	($\mu\text{mol m}^{-2}$ dry soil)		
1	265	352.5	15.2	72.7	18.4	12.7
2	213.3	234.2	29.1	181.7	10.4	7.2
3	260	na	-35.2	na	12.1	8.4
4	388.3	35.8	-193.3	335	20.9	14.5
5	334.2	56.7	25.2	135	19.0	13.2
6	501.7	87.5	8.3	283.3	19.3	13.4

637

638 **Figure legends**

639

640 **Figure 1:** Excess ^{13}C of shoot-respired CO_2 (a) and of soil-respired CO_2 (b) after ^{13}C pulse-
641 labelling for six pots with soil-wheat plant systems, plants representing a wide
642 ecophysiological range (see Table 1).

643

644 **Figure 2:** Relationship between stomatal conductance and the initial slope of excess ^{13}C in
645 shoot-respired CO_2 (excess $^{13}\text{C}_{\text{R-shoot}}$) after ^{13}C labelling (a) as well as the time until maximum
646 peak of excess ^{13}C of soil-respired CO_2 (excess $^{13}\text{C}_{\text{R-soil}}$) is reached after ^{13}C labelling (b) for
647 six pots with soil-wheat plant systems, plants representing a wide ecophysiological range (see
648 Table 1). Linear regressions were highly significant (a: $y=-0.022x-0.015$, $p=0.029$, $R^2=0.73$;
649 b: $y=-13.5x+23.4$, $p=0.023$, $R^2=0.76$).

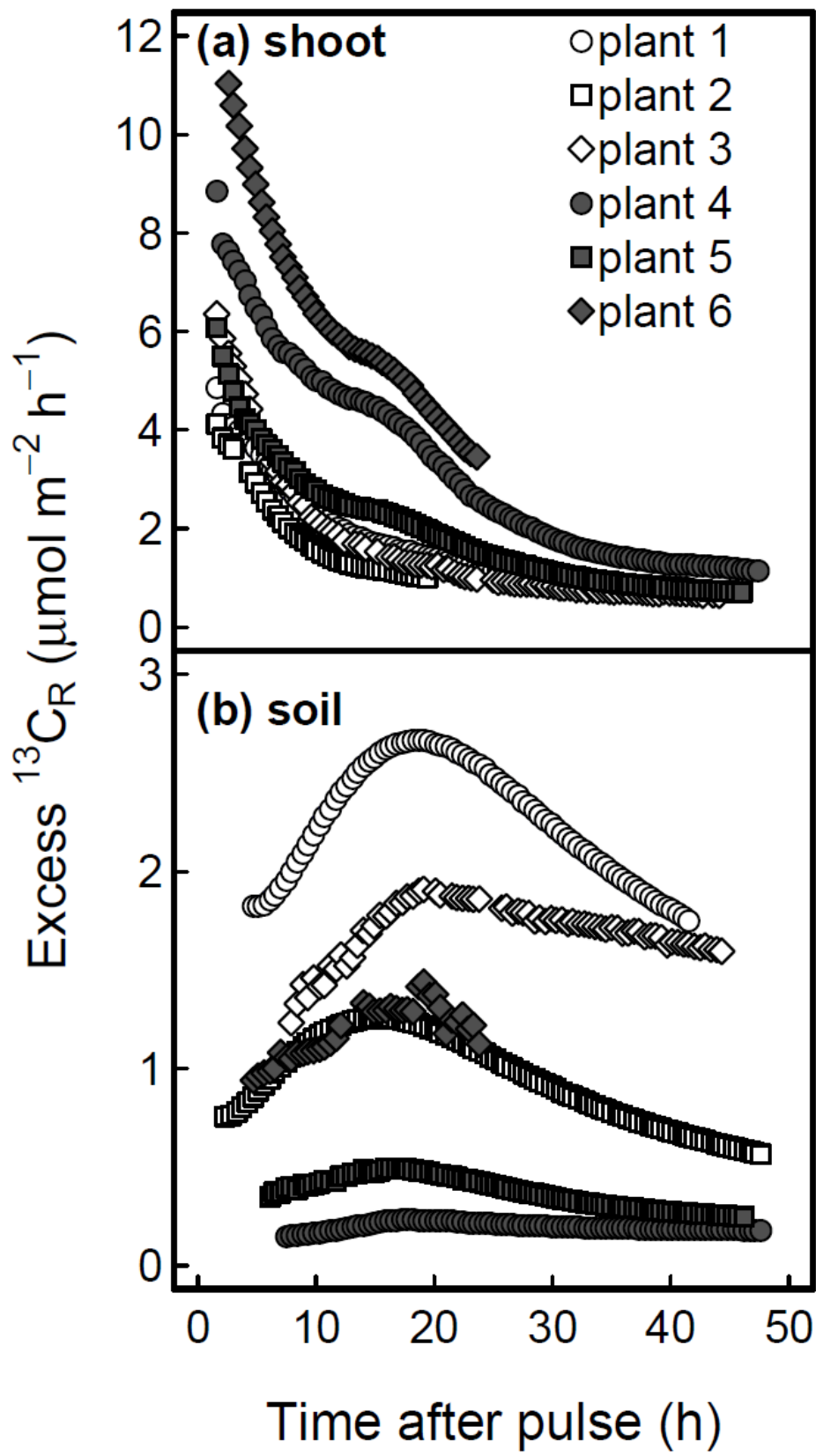
650

651 **Figure 3:** Relationship between N concentration in soil and root and maximum excess $^{13}\text{C}_{\text{R-}}$
652 soil after labelling (a and b, respectively) as well as total excess $^{13}\text{C}_{\text{R-soil}}$ after labelling (c and
653 d, respectively), for six pots with soil-wheat plant systems (see Table 1). Linear regressions
654 were significant for soil N concentration (a: $y=-123.40x+119.26$, $p=0.045$, $R^2=0.67$; c: $y=-$
655 $3785.30x+3544.60$, $p=0.030$, $R^2=0.73$) and marginally significant for root N concentration (b:
656 $y=-21.90x+80.50$, $p=0.052$, $R^2=0.65$; d: $y=-637.80x+2295.30$, $p=0.055$, $R^2=0.64$).

657

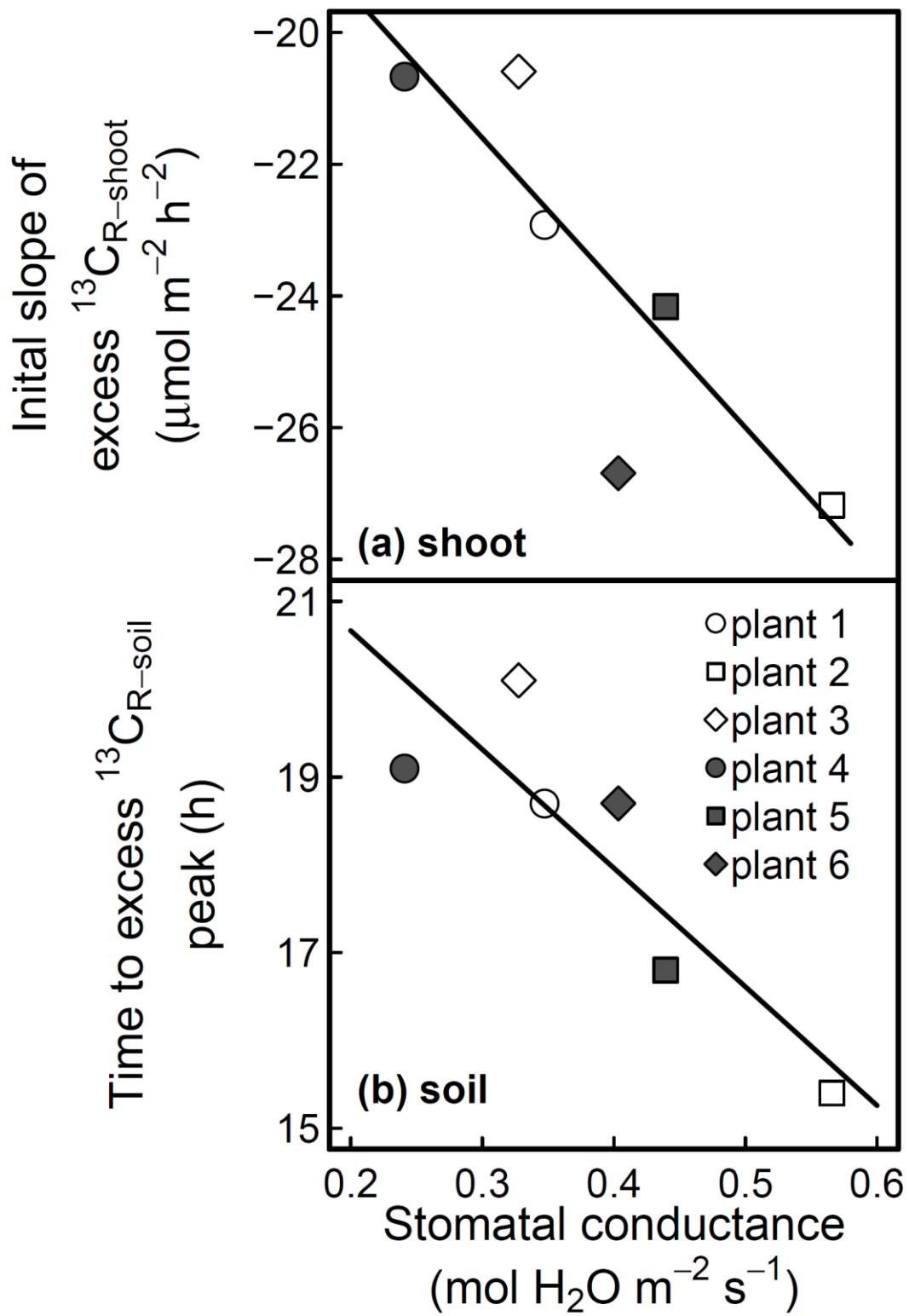
658 **Figure 4:** Relationship between excess ^{13}C in the root compartment and maximum excess ^{13}C
659 in soil-respired CO_2 after ^{13}C labelling (excess $^{13}\text{C}_{\text{R-soil}}$, a) as well total excess $^{13}\text{C}_{\text{R-soil}}$ after
660 labelling (b) for six pots with soil-wheat plant systems (see Table 1). Linear regressions were
661 significant (a: $y=0.19x+0.08$, $p=0.039$, $R^2=0.80$; b: $y=5.80x+1.58$, $p=0.025$, $R^2=0.85$).

662



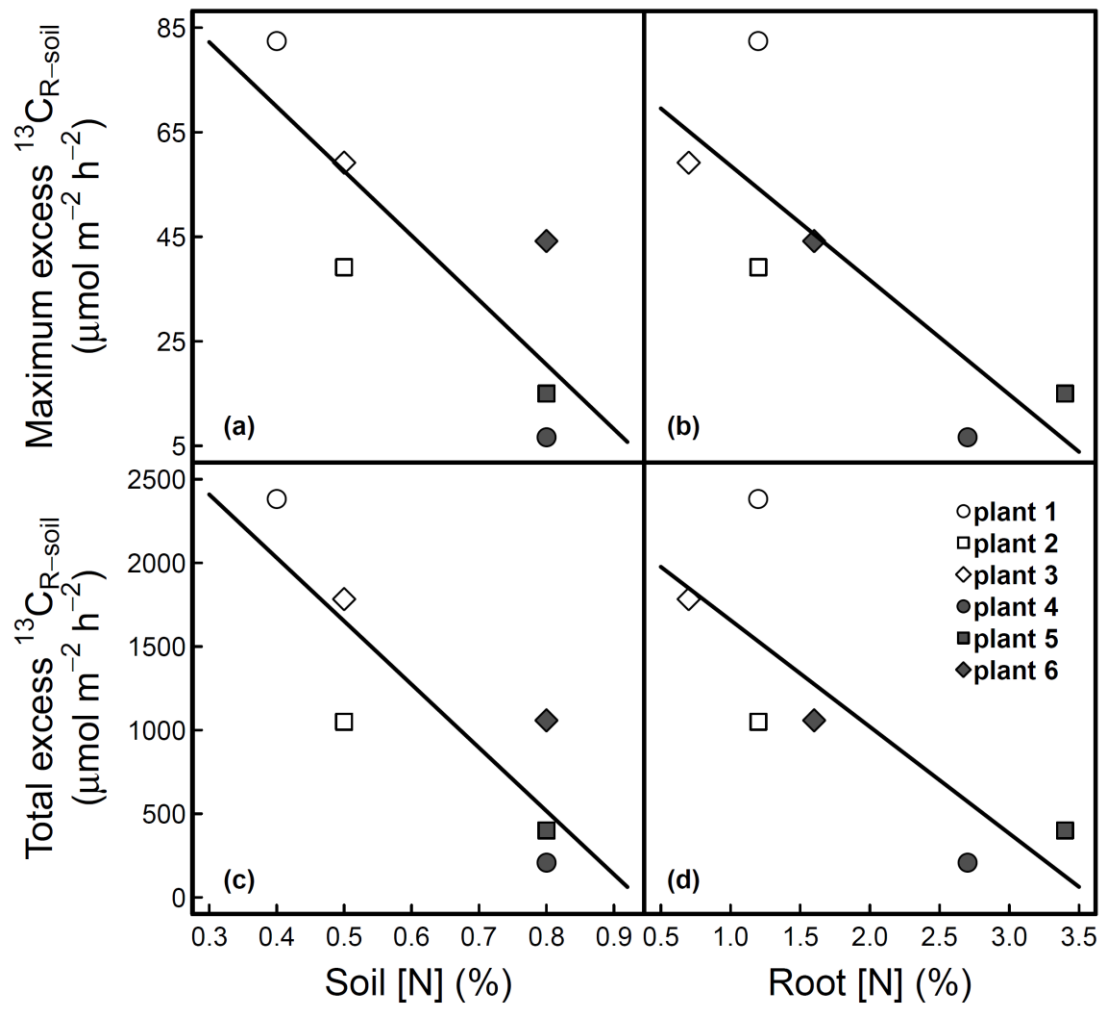
663 Figure 1

664



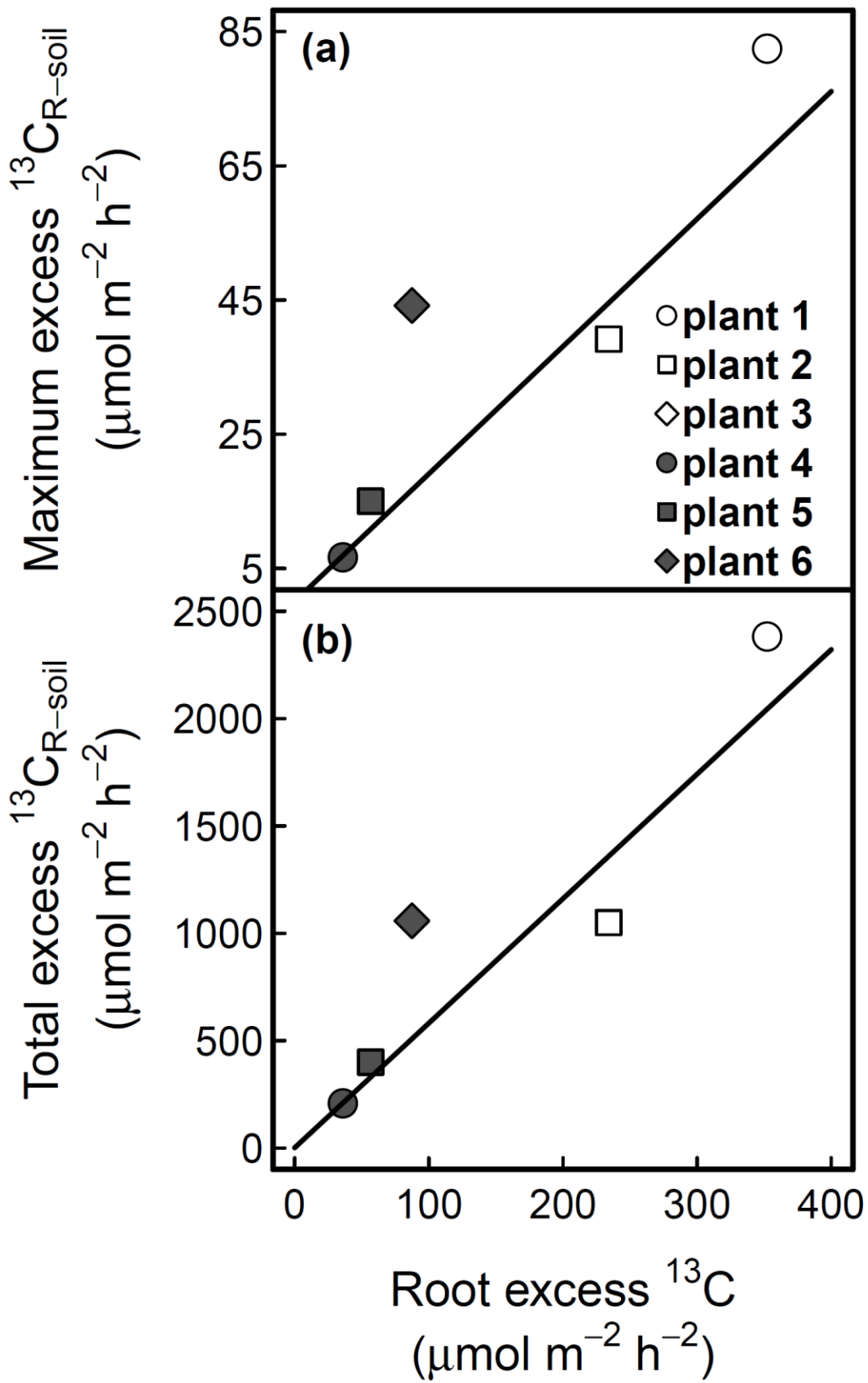
665 Figure 2

666



667 Figure 3

668



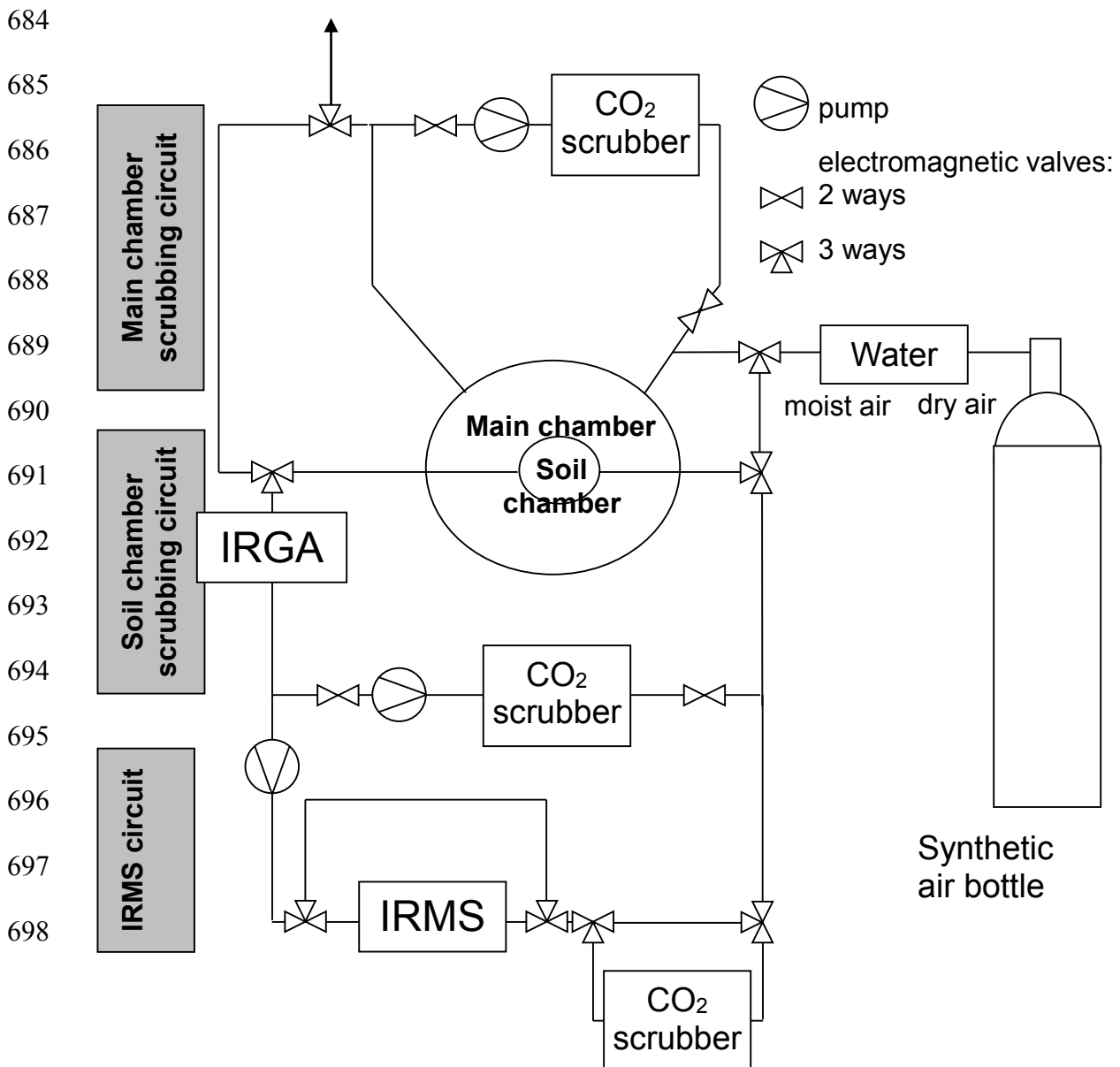
669 Figure 4

670

671 **Supplementary material**

672 Custom-built setup for online IRMS measurements used to monitor $\delta^{13}\text{C}$ of respired
 673 CO_2 in main and soil chambers.

674 Air flow through the setup was controlled by a computer and electro-valves. The
 675 IRMS air intake circuit was connected alternatively to the soil chamber circuit or to the main
 676 chamber circuit, which were independently equipped with a pump and a CO_2 scrubber (soda
 677 lime). The IRMS circuit featured a membrane pump (1 L min^{-1} flow rate) and a scrubber,
 678 maintaining CO_2 concentrations below 1000 $\mu\text{mol mol}^{-1}$. Before each measurement, CO_2 was
 679 scrubbed from all circuits and chambers. CO_2 concentrations were then left to increase due to
 680 respiration to at least 300 $\mu\text{mol CO}_2 \text{ mol}^{-1}$ before directing the air flow to the IRMS. The 300
 681 and 1000 $\mu\text{mol CO}_2 \text{ mol}^{-1}$ thresholds ensured optimal CO_2 concentrations for $\delta^{13}\text{C}$
 682 measurements. CO_2 and H_2O concentrations were measured with a $\text{CO}_2/\text{H}_2\text{O}$ gas analyzer
 683 (Li-840, Li-Cor Inc.) placed in the part shared by both soil and main circuits.



699 Air flow for online measurements of $\delta^{13}\text{C}$ in CO_2 . EV, IRGA and IRMS indicate electro-
700 valves, infra-red gas analyser and isotope ratio mass spectrometer, respectively. The soil
701 chamber is located inside the main chamber; both are independently connected to the IRMS
702 and IRGA circuits.